2011

Synthesis and Physicochemical Properties of Cationic Microgels Based on Poly(N-isopropylmethacrylamide)

Xiaobo Hu
Georgia Institute of Technology

Zhen Tong
South China University of Technology

L. Andrew Lyon
Chapman University, lyon@chapman.edu

Recommended Citation
Hu, X. B.; Tong, Z.; Lyon, L. A., Synthesis and physicochemical properties of cationic microgels based on poly(N-isopropylmethacrylamide), *Colloid and Polymer Science* 2011, 289(3), 333-339. doi: 10.1007/s00396-010-2347-y

Synthesis and Physicochemical Properties of Cationic Microgels Based on Poly(N-isopropylmethacrylamide)

Published in final edited form as:
Colloid Polym Sci. 2010 December 4; 289(3): 333–339. doi:10.1007/s00396-010-2347-y.

Synthesis and Physicochemical Properties of Cationic Microgels Based on Poly(*N*-isopropylmethacrylamide)

Xiaobo Hu[a,b], **Zhen Tong**[b], and **L. Andrew Lyon**[a,*]

[a] School of Chemistry & Biochemistry and the Petit Institute for Bioengineering & Bioscience, Georgia Institute of Technology, Atlanta, GA 30332, USA

[b] Research Institute of Materials Science, South China University of Technology, Guangzhou 510640, P.R. China

Abstract

Surfactant-free, radical precipitation co-polymerization of *N*-isopropylmethacrylamide (NIPMAm) and the cationic co-monomer *N*-(3-aminopropyl) methacrylamide hydrochloride (APMH) was carried out to prepare microgels functionalized with primary amines. The morphology and hydrodynamic diameter of the microgels were characterized by atomic force microscopy (AFM) and photon correlation spectroscopy (PCS), with the effect of NaCl concentration and initiator type on the microgel size and yield being investigated. When a V50-initiated reaction was carried out in pure water, relatively small microgels (~160 nm diameter) were obtained in low yield (~20%). However, both the yield and size increased if the reaction was carried out in saline or by using APS as initiator instead of V50. Stable amine-laden microgels in the range from 160 nm to 950 nm in diameter with narrow size distributions were thus produced using reaction media with controlled salinity. Microgel swelling and electrophoretic mobility values as a function of pH, ionic strength and temperature were also studied, illustrating the presence of cationic sidechains and their influence on microgel properties. Finally, the availability of the primary amine groups for post-polymerization modification was confirmed via modification with fluorescein-NHS.

Keywords

Controlled salinity; Microgel; N-isopropylmethacrylamide; cationic polymer

Introduction

Temperature-sensitive poly(*N*-isopropylacrylamide) (pNIPAm) microgels, which were first prepared by emulsion polymerization in 1986 [1], have received a significant amount of attention due to dramatic changes in physicochemical properties observed when temperature is raised above their volume phase transition temperature (VPTT, ~31 °C). In recent years, such microgels have been used in drug delivery [2–4], biosensors [5–7], tissue regeneration [8,9], and chemical separations [10]. In many of these applications, the introduction of specific chemical functionalities is desired, such that the polymer can be elaborated upon following synthesis. Toward that end, functionalities such as carboxyl [11], azido [12] and glycidyl [13] groups have been copolymerized into pNIPAm microgels. However, the primary amine, a reactive group that is particularly useful for bioconjugation [14], has been far less studied in microgel synthesis. The utility of this group is associated with the potential for binding with anionic moieties on oligonucleotides, proteins, or enzymes [14–

*To whom correspondence should be addressed. lyon@gatech.edu.

16], as well as its use in the covalent attachment to molecules carrying isothiocyanates or succinimidyl esters.

Given the utility of amine chemoligation sites, the incorporation of amines into microgels has been studied in a few cases. Xu et al. prepared primary amine functionalized pNIPAm microgels by copolymerization of *N*-isopropylacrylamide (NIPAm) with *N*-vinylformamide (NVF) by a semi-batch route, followed by conversion of the formamide moieties to a primary amine by acid hydrolysis [17]. Unfortunately, this method requires multiple steps and very strong acid hydrolysis conditions, thereby limiting its broad application. Leung et al. prepared microgels by graft copolymerization of NIPAm from either PEI or chitosan, which results in core-shell structures with the amines mainly becoming shell-localized [18]. This approach produces a very thin polymer shell, with the amine concentration being limited due to the stabilization effect of polymer during the synthesis. Meunier et al. prepared amine-laden pNIPAm microgels by using 2,2′-azobis (2-amidinopropane) dihydrochloride (V50) as initiator and 2-aminoethylmethacrylate hydrochloride (AEMH) as a functional monomer [19]. However, the ester group in the AEMH monomer can be easily hydrolyzed to carboxyl during the synthesis because of the acid solution and high temperature, which can cause these microgels to be unstable. In this paper, we discuss alternate routes for the preparation of amine functionalized microgels based on poly(*N*-isopropylmethacrylamide) (pNIPMAm). The use of pNIPMAm, which has a volume phase transition temperature of ~43 °C was motivated by our recent use of this polymer in drug delivery applications [4]. Thus, we are very interested in broadening the utility of those particular microgels by increasing the range of functionalities that can be efficiently incorporated.

Experimental

Materials

All materials were purchased from Sigma-Aldrich unless otherwise noted. The monomer *N*-isopropylmethacrylamide (NIPMAm) was recrystallized from *n*-hexane (J. T. Baker). Comonomer *N*-(3-aminopropyl)methacrylamide hydrochloride (APMH, Polysciences Inc.), cross-linker *N*,*N*′-methylene(bisacrylamide) (BIS), cationic initiator 2,2′-azobis(2-amidinopropane) dihydrochloride (V50) and anionic initiator ammonium persulfate (APS) were all used as received. NHS-Fluorescein (Thermo Sci.) and NaCl were used as received. Pure water was produced by deionization to a resistance of 18 MΩ·cm (Barnstead E-Pure system), followed by filtration through a 0.2-μm filter to remove particulate matter.

Microgel Synthesis

Microgels were synthesized by surfactant-free, radical precipitation co-polymerization using methods similar to those previously reported [20]. For all reactions, the molar composition was 89% NIPMAm, 9% APMH, and 2% BIS, with a total monomer concentration of 140 mM (Table 1). In a typical synthesis, 50 mL of a filtered, aqueous solution of NIPMAm, APMH, BIS and NaCl was added to the reaction flask, which was then heated to 70 °C. The solution was purged with N_2 gas with continuous stirring until the temperature remained stable. The reaction was initiated by addition of 2 mL of a V50 or APS solution. The reaction was allowed to continue for 20 h while being purged by N_2 gas with constant stirring. After synthesis, the solution was filtered through glass wool to remove any coagulum and then centrifuged/redispersed several times for purification. After purification, the microgel dispersion was lyophilized for at least 72 hours.

Atomic Force Microscopy (AFM)

Microgels were imaged using an Asylum Research MFP-3D Instrument (Santa Barbara, CA). Imaging was performed and processed using the MFP-3D software under the IgorPro (WaveMetrics Inc., Lake Oswego, OR) environment. Non-contact mode aluminum-coated silicon nitride cantilevers were purchased from NanoWorld (force constant = 42 N/m, resonant frequency = 320 kHz). All images were taken in air under ambient conditions. AFM samples were prepared by centrifugal deposition at a maximum rotor speed of 2250 × *g* for 5 min on glass coverslips [21]. Glass coverslips (22 mm × 22 mm) were cleaned using an air plasma (Harrick Plasma, Ithaca, NY) for ~ 15 min. Each cleaned slide was functionalized by exposure to a 1% solution of 3-aminopropyltrimethoxysilane (APTMS) in absolute ethanol (200 proof) for ~3 h. The glass was then rinsed with ethanol and dried under a gentle stream of N_2. The amine-functionalized coverslips were further modified by immersion in a 0.1 mg/mL poly(sodium styrenesulfonate) solution before the centrifugal deposition of microgels. After microgel deposition, the sample was gently rinsed with deionized water and dried under a gentle stream of N_2.

Particle size characterization

Particle sizes were determined by photon correlation spectroscopy (PCS; Protein Solutions, Inc.) using an instrument equipped with an integrated Peltier temperature control device, which provides temperature accuracy within ±0.1 °C. The instrument collects scattering light at 90° by a single-mode optical fiber coupled to an avalanche photodiode detector. The samples were thermally equilibrated at each temperature for 30 min before each measurement. The data presented are the averaged values of 20 measurements, with a 10 s integration time for each measurement.

Zeta-potential Determination

The ζ-potential was measured with a Zetasizer Nano-ZS (Malvern). Before the measurements, the 1 mL microgel dispersion in the designated buffer was thermally equilibrated between parallel electrodes in cuvette for 10 min. The ζ-potential value was the average of at least three successive measurements.

Fluorescence labeling and imaging

For conjugating the amine reactive fluorescein, 2.5 mg of amine microgels were dispersed in 5 mL of a pH 7.4 PBS buffer, and 1.6 mL of 1 mg/mL DMF solution of fluorescein-NHS was added. The solution was stirred at 4 °C overnight and then purified by dialysis against DI water for ~2 weeks with the water being changed twice per day, using Spectra-Pro 10,000 MW cut-off dialysis tubing (VWR). The dyed microgels were imaged by fluorescence microscopy, which was conducted on an Olympus IX-70 inverted microscope equipped with a high numerical aperture, oil immersion 100 × objective (NA = 1.30). The excitation irradiation was a mercury lamp filtered by excitation band-pass filters of 450–490 nm. Images were captured using a color CCD camera (PixelFly, Cooke Corporation).

Results and Discussion

During the preparation of pNIPAm or pNIPMAm microgels, an anionic initiator APS or cationic initiator V50 is typically degraded thermally to initiate the polymerization, which results in anionic or cationic microgels, respectively [1,22]. During our experiments, initial attempts to prepare poly(NIPMAm-*co*-APMH) microgels (μG) in pure water using a cationic initiator (V50) resulted in microgels of a very small size with poor yield (Table 1). A possible reason for the poor yield lies in unfavorable reactivity ratio between the two co-monomers, which inhibits the formation of copolymer chains that can easily collapse at high

temperature [23]. Randomly positioned APMH along the copolymer chain creates sufficiently strong Coulombic repulsion between the cationic groups such that thermo-induced chain collapse is inhibited. A similar phenomenon has been described previously by Meunier et al., where high AEMH concentrations accelerated the incorporation rate of BIS during particle formation, making the capture of polymer formed later in the reaction unfavorable [19]. As a result, many free polymer chains may be formed instead of collapsed precursor particles, thereby reducing the yield of microgels, and limiting the subsequent polymer size due to a decrease in the amount of incorporated polymer/particle. Fortunately, the reactivity ratio of ionic monomers can be notably influenced by the ionic strength [23,24]. We therefore investigated the influence of NaCl concentration on microgel preparation.

From Table 1, we can see that the diameter of μG0 microgels in pH 3 buffer (10 mM) is ~715 nm, with a yield of ~45%. However, the particle diameter decreased to ~157 nm after the addition of 9 mol% APMH, with the yield of cross-linked microgels dropping to 20%. In the past, the presence of salt in alkylacrylamide emulsion polymerization media has been avoided due to the propensity of deswollen particles to aggregate under high salinity conditions [25]. However, in this study, our results show that increasing the salinity of the reaction medium increases the microgel size along with a modest increase in microgel yield. We hypothesize that the salt affects the polymerization in at least two ways. After the addition of NaCl, the Coulombic repulsion between the positively charged APMH units becomes sufficiently screened to allow a greater tendency for homopropagation, which will result in polymers with a longer sequence of APMH units in the copolymer chains. The block-like copolymer chains will undergo thermally-induced collapse more readily, as has been observed for other block copolymers containing pNIPAm [26]. Consequently, more polymer chains will become incorporated into the growing microgels instead of remaining in solution as uncrosslinked “free” polymer chains. Additionally, it is likely that growing microgels will undergo aggregation with the other precursor particles under these charge-shielding conditions, thereby producing a larger average particle size. However, when the NaCl concentration reached 200 mM, the reaction system became unstable and macroscopic coagulation of the polymer was observed.

In addition to the impact of salinity on microgel formation, the influence of different initiators was studied, where the anionic initiator APS was used to initiate the polymerization instead of V50. Despite the obvious potential for forming zwitterionic microgels when APS is used, no colloidal instability was observed during the syntheses undertaken in this work. Particles produced under the conditions for μG5 had a diameter of ~500 nm with a yield of 60%, which is much higher than that obtained from the corresponding V50 synthesis. When the APS concentration was increased to 2 mM, a particle diameter of 740 nm and 65% yield was obtained (μG6). Whereas these results are too preliminary to completely explain this phenomenon, we tentatively ascribe these results to the presence of the oxygen-centered radical associated with APS, which is more effective in abstracting a hydrogen atom from the carbon next to the amine group in APMH. This chain transfer reaction will provide additional reactive sites, which will induce continuous graft polymerization and self cross-linking [27,28], resulting in larger microgels and higher polymer yields.

The ζ-potentials of the microgels in pure water are listed in Table 1; all microgels display a positive ζ-potential indicating cationic character. For μG0 and μG1, the ζ-potentials are of similarly low magnitude. For μG0, the positive charge is due to the amidine end groups arising from the V50 initiator. The lack of a significant change in this value for μG1, which was synthesized using 9 mol% APMH, suggests that the degree of APMH incorporation was very poor. In contrast, there is a large increase in the ζ-potential value for microgels

synthesized with increasing salinity or with APS as the initiator, which is indicative of surface charges imparted by more efficient incorporation of APMH. It is also interesting to note that μG6 displays a slightly higher zeta-potential than the other samples, even though this particle must also contain some anionic initiator residues. This, coupled with the observation that these conditions display the highest yield, suggests that APMH incorporation is maximized for μG6 relative to the other conditions.

Analysis of the microgels via AFM permits visualization of the particle morphology and polydispersity estimation (Figure 1). It should be noted that in all cases, the strong microgel-surface interactions, combined with the fact that the particles are dehydrated, result in severely flattened particles. Of particular interest in these data is the observation that μG3 and μG4 do not appear to be purely spherical particles. Instead, these microgels appear somewhat irregular and “bumpy”, as if formed via the aggregation of multiple smaller particles. Such precursor particle aggregation would be predicted to occur more readily in high salt. Alternatively, the addition of NaCl likely results in the formation of block-like copolymers during the microgel synthesis [23,24], as described above. If this is indeed the case, the resultant particles might contain relatively long polyelectrolyte chains at the microgel surface. This shell-localized polymer will randomly spread on the substrate during the drying process, resulting in a non-spherical particle appearance. Conversely, microgels μG5 and μG6 appear spherical, which perhaps suggests a homogeneous particle architecture. Line profiles taken from these images permit estimation of the dried microgel heights and diameters. The height/diameter ratio provides a rough, qualitative estimate of microgels stiffness [29]; this analysis suggests that the APS-initiated microgels (μG5 and μG6) are somewhat stiffer than those prepared with V50 (Figure 1f), presumably due to increased cross-linking brought about by the aforementioned chain transfer reactions.

In addition to microgel morphology, it is critical to know how the different synthetic conditions impact the temperature and pH dependent swelling and charge characteristics. The physicochemical properties of selected microgels are summarized in Figure 2. As expected from their pNIPMAm content, all microgels display a volume phase transition temperature (VPTT) between 40 and 50 °C (Figure 2a). Those lacking cationic co-monomer (μG0) display a transition very close to the LCST of pure pNIPMAm (~44 °C), with the VPTT of all other microgels being shifted to higher temperatures, as is typical for microgels containing hydrophilic or charged groups [30,31]. The swelling ratio is also presumably influenced by the presence of charged co-monomers (Figure 2b), as the swelling ratios of the amine containing microgels are all smaller than that of μG0. Amine incorporation is also evident in the influence of ionic strength on the measured microgel size at pH 3 (Figure 2c). Below the VPTT, the diameter of μG3 is observed to decrease as the ionic strength increased from 2 mM to 100 mM. Furthermore, the VPTT is shifted to lower temperatures with a concomitant sharpening of the transition. These effects arise largely from charge screening, competitive solvation, and osmotic effects [25,32,33]. By measuring the microgel swelling ratio as a function of pH (defined as the ratio of the microgel diameter at a particular pH relative to that at pH 11.5), we observe the expected result that the swelling ratio gradually decreases at pH values higher than 7.4 and plateaus above the pKa (~10) of APMH (Figure 2d). The pH dependence of the ζ-potential closely mirrors the swelling data (Figure 2e), where in the absence of APMH (μG0), no pH dependence is observed, but a strong pH effect is observed in the presence of APMH (μG3 and μG6). For the APMH containing microgels, the ζ-potential decreases as the pH increases. For example, the ζ-potential of μG6 suddenly decreases with a pH change from 9.5 to 10.5, with this pH corresponding to the pKa of primary amine group. However, for μG3, the ζ-potential gradually decreases once the pH increases above 7.4. This difference in pKa between the polyelectrolyte and the parent monomer is common due to the decreased propensity for deprotonation in the presence of the neighboring ionic groups [34]. For example, poly(2-aminoethyl methacrylate), which has

a similar structure to pAPMH, has a pKa of approximately 7.6. This pKa is significantly lower than that of its monomer (pKa =10) [35]. This result is therefore also suggests that the addition of NaCl results in the formation of block-like copolymers. Due to the cationic initiator fragments, the ζ-potential is always positive for the μG0 and μG3 microgels over the pH range studied here. However, due to the neutralization of the amine sidechains and the presence of anionic initiator groups, the ζ-potential of μG6 microgels is negative at pH 11.5. Finally, to illustrate that the amine groups are accessible to small molecule coupling reactions, fluorescein-NHS was used as a coupling probe for microgels μG3 and μG6; a representative image of μG6 is shown (Figure 2f). Studies investigating the accessibility of those groups in a wider range of bioconjugation reactions are currently underway.

Conclusions

In this investigation, we have shown that primary amine containing pNIPMAm microgels can be produced by a surfactant free radical precipitation copolymerization. By controlling the reaction salinity or using an anionic initiator APS, low polydispersity, primary amine containing pNIPMAm microgels can be obtained in high yield. The increase of particle size and yield by the salt addition originates from the screening of Coulombic repulsion between APMH units, which results in more favorable polymer incorporation. The resultant amine-laden microgels show the expected swelling properties of thermoresponsive cationic microgels as a function of temperature, pH and ionic strength, as well as reactivity in standard amide bond-forming reactions. Studies of these microgels in the context of biomolecule conjugation and thin film self-assembly are currently underway.

Acknowledgments

This work was partially supported by the National Institutes of Health (1 R01 GM088291-01). XH thanks China Scholarship Council (CSC) for fellowship support. We thank the Kröger group at GT for the use of their zeta potential equipment.

References

1. Pelton RH, Chibante P. Preparation of Aqueous Lattices with N-Isopropylacrylamide. Colloids and Surfaces. 1986; 20:247–256.
2. Lee CF, Lin CC, Chi WY. Thermosensitive and control release behavior of poly (N-isopropylacrylamide-co-acrylic acid) latex particles. Journal of Polymer Science Part a-Polymer Chemistry. 2008; 46:5734–5741.
3. Choi SH, Yoon JJ, Park TG. Galactosylated poly(N-isopropylacrylamide) hydrogel submicrometer particles for specific cellular uptake within hepatocytes. Journal of Colloid and Interface Science. 2002; 251:57–63. [PubMed: 16290701]
4. Blackburn WH, Dickerson EB, Smith MH, McDonald JF, Lyon LA. Peptide-Functionalized Nanogels for Targeted siRNA Delivery. Bioconjugate Chemistry. 2009; 20:960–968. [PubMed: 19341276]
5. Kim J, Nayak S, Lyon LA. Bioresponsive hydrogel microlenses. Journal of the American Chemical Society. 2005; 127:9588–9592. [PubMed: 15984886]
6. Kim JS, Singh N, Lyon LA. Displacement-induced switching rates of bioresponsive hydrogel microlenses. Chemistry of Materials. 2007; 19:2527–2532.
7. Zhang YJ, Guan Y, Zhou SQ. Synthesis and volume phase transitions of glucose-sensitive microgels. Biomacromolecules. 2006; 7:3196–3201. [PubMed: 17096551]
8. Jia XQ, Yeo Y, Clifton RJ, Jiao T, Kohane DS, Kobler JB, Zeitels SM, Langer R. Hyaluronic acid-based microgels and microgel networks for vocal fold regeneration. Biomacromolecules. 2006; 7:3336–3344. [PubMed: 17154461]
9. Freemont TJ, Saunders BR. PH-responsive microgel dispersions for repairing damaged load-bearing soft tissue. Soft Matter. 2008; 4:919–924.

10. Grabstain V, Bianco-Peled H. Mechanisms controlling the temperature-dependent binding of proteins to poly(N-isopropylacrylamide) microgels. Biotechnology Progress. 2003; 19:1728–1733. [PubMed: 14656148]
11. Snowden MJ, Chowdhry BZ, Vincent B, Morris GE. Colloidal copolymer microgels of N-isopropylacrylamide and acrylic acid: pH, ionic strength and temperature effects. Journal of the Chemical Society-Faraday Transactions. 1996; 92:5013–5016.
12. Meng ZY, Hendrickson GR, Lyon LA. Simultaneous Orthogonal Chemoligations on Multiresponsive Microgels. Macromolecules. 2009; 42:7664–7669.
13. Suzuki D, Kawaguchi H. Hybrid microgels with reversibly changeable multiple brilliant color. Langmuir. 2006; 22:3818–3822. [PubMed: 16584261]
14. Hermanson, GT. Bioconjugate Techniques. Academic Press; San Diego: 1995.
15. Dyer MA, Ainslie KM, Pishko MV. Protein adhesion on silicon-supported hyperbranched poly(ethylene glycol) and poly(allylamine) thin films. Langmuir. 2007; 23:7018–7023. [PubMed: 17506587]
16. Ramos J, Martin-Molina A, Sanz-Izquierdo MP, Rus A, Borque L, Hidalgo-Alvarez R, Galisteo-Gonzalez F, Forcada J. Amino-functionalized latex particles obtained by a multistep method: Development of a new immunoreagent. Journal of Polymer Science Part a-Polymer Chemistry. 2003; 41:2404–2411.
17. Xu JJ, Timmons AB, Pelton R. N-Vinylformamide as a route to amine-containing latexes and microgels. Colloid and Polymer Science. 2004; 282:256–263.
18. Leung MF, Zhu JM, Harris FW, Li P. New route to smart core-shell polymeric microgels: Synthesis and properties. Macromolecular Rapid Communications. 2004; 25:1819–1823.
19. Meunier F, Elaissari A, Pichot C. Preparation and Characterization of Cationic Poly(N-Isopropylacrylamide) Copolymer Latexes. Polymers for Advanced Technologies. 1995; 6:489–496.
20. Meng Z, Cho JK, Breedveld V, Lyon LA. Physical Aging and Phase Behavior of Multiresponsive Microgel Colloidal Dispersions. Journal of Physical Chemistry B. 2009; 113:4590–4599.
21. South AB, Whitmire RE, Garcia AJ, Lyon LA. Centrifugal Deposition of Microgels for the Rapid Assembly of Nonfouling Thin Films. Acs Applied Materials & Interfaces. 2009; 1:2747–2754. [PubMed: 20356152]
22. Bao LY, Zha LS. Preparation of poly(N-isopropylacrylamide) microgels using different initiators under various pH values. Journal of Macromolecular Science Part a-Pure and Applied Chemistry. 2006; 43:1765–1771.
23. Mai-ngam K, Boonkitpattarakul K, Sakulsombat M, Chumningan P, Mai-ngam B. Synthesis and phase separation of amine-functional temperature responsive copolymers based on poly(N-isopropylacrylamide). European Polymer Journal. 2009; 45:1260–1269.
24. Bokias G, Hourdet D. Synthesis and characterization of positively charged amphiphilic water soluble polymers based on poly(N-isopropylacrylamide). Polymer. 2001; 42:6329–6337.
25. Lopez-Leon T, Ortega-Vinuesa JL, Bastos-Gonzalez D, Elaissari A. Cationic and anionic poly(N-isopropylacrylamide) based submicron gel particles: Electrokinetic properties and colloidal stability. Journal of Physical Chemistry B. 2006; 110:4629–4636.
26. Zhao JP, Zhang GZ, Pispas S. Morphological Transitions in Aggregates of Thermosensitive Poly(ethylene oxide)-b-poly(N-isopropylacrylamide) Block Copolymers Prepared via RAFT Polymerization. Journal of Polymer Science Part a-Polymer Chemistry. 2009; 47:4099–4110.
27. Gao J, Frisken BJ. Cross-linker-free N-isopropylacrylamide gel nanospheres. Langmuir. 2003; 19:5212–5216.
28. Gao J, Frisken BJ. Influence of secondary components on the synthesis of self-cross-linked N-isopropylacrylamide microgels. Langmuir. 2005; 21:545–551. [PubMed: 15641822]
29. Huang X, Misra GP, Vaish A, Flanagan JM, Sutermaster B, Lowe TL. Novel Nanogels with Both Thermoresponsive and Hydrolytically Degradable Properties. Macromolecules. 2008; 41:8339–8345.
30. Ma XM, Xi JY, Xian Z, Tang XZ. Deswelling comparison of temperature-sensitive poly(N-isopropylacrylamide) microgels containing functional-OH groups with different hydrophilic long side chains. Journal of Polymer Science Part B-Polymer Physics. 2005; 43:3575–3583.

31. Debord JD, Lyon LA. Synthesis and characterization of pH-responsive copolymer microgels with tunable volume phase transition temperatures. Langmuir. 2003; 19:7662–7664.
32. Daly E, Saunders BR. A study of the effect of electrolyte on the swelling and stability of poly(N-isopropylacrylamide) microgel dispersions. Langmuir. 2000; 16:5546–5552.
33. Fernandez-Nieves A, Fernandez-Barbero A, de las Nieves FJ. Salt effects over the swelling of ionized mesoscopic gels. Journal of Chemical Physics. 2001; 115:7644–7649.
34. van de Wetering P, Zuidam NJ, van Steenbergen MJ, van der Houwen OAGJ, Underberg WJM, Hennink WE. A mechanistic study of the hydrolytic stability of poly(2-(dimethylamino)ethyl methacrylate). Macromolecules. 1998; 31:8063–8068.
35. Thompson KL, Read ES, Armes SP. Chemical degradation of poly(2-aminoethyl methacrylate). Polymer Degradation and Stability. 2008; 93:1460–1466.

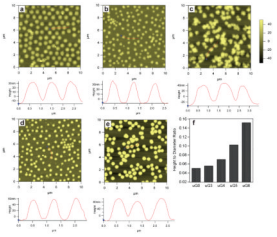

Figure 1.
AFM height images and line profiles of (a) μG0, (b) μG3, (c) μG4, (d) μG5, and (e) μG6. (f) Histogram of calculated height/diameter ratios.

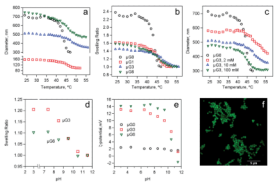

Figure 2.

(a) Hydrodynamic diameter and (b) swelling ratio vs. T of the indicated microgels in pH 3 buffer (I = 10 mM). (c) Diameter vs. T for μG3 microgels in pH 3 buffers with different ionic strengths. μG0 microgels in pH 3 (10 mM) is shown for comparison. The dependence of: (d) swelling ratio and (e) ζ-potential of the indicated microgels as a function of pH with the ionic strength held constant at 2 mM. (f) Fluorescence microscopy image of fluorescein-labeled μG6 microgels.

Table 1

Synthesis conditions, yields, and microgel properties.

Code[a]	APMH/mol %	V50/mM	APS/mM	[NaCl]/mM	D_h/nm[b]	ζ-potential in DI water/mV	Yield/%
μG0	0	2	-	0	714	13.4	45
μG1	9	2	-	0	157	12.9	20
μG2	9	2	-	50	318	33.8	25
μG3	9	2	-	100	508	37.8	35
μG4	9	2	-	150	950	38.9	38
μG5	9	-	1	0	498	33.8	60
μG6	9	-	2	0	744	41.7	65

[a]Reaction conditions: total monomer concentration = 140 mM, temperature = 70 °C, reaction time: 20 h.

[b]Solution conditions: pH 3, 10 mM ionic strength.

Colloid Polym Sci. Author manuscript; available in PMC 2011 March 16.